

Isospin dependence of nuclear multifragmentation in $^{112}\text{Sn}+^{112}\text{Sn}$ and $^{124}\text{Sn}+^{124}\text{Sn}$ collisions at 40 MeV/nucleon

Feng-Shou Zhang,^{1,2,3} Lie-Wen Chen,^{1,2} Zhao-Yu Ming,^{1,2} and Zhi-Yuan Zhu^{1,4}¹Center of Theoretical Nuclear Physics, National Laboratory of Heavy Ion Accelerator, Lanzhou 730000, China²Institute of Modern Physics, Academia Sinica, P.O. Box 31, Lanzhou 730000, China³CCAST (World Laboratory), P.O. Box 8730, Beijing 100080, China⁴Shanghai Institute of Nuclear Research, Academia Sinica, Shanghai 201800, China

(Received 17 May 1999; published 9 November 1999)

Within the framework of an isospin-dependent quantum molecular dynamics model, the multifragmentation in reactions of $^{112}\text{Sn}+^{112}\text{Sn}$ and $^{124}\text{Sn}+^{124}\text{Sn}$ at 40 MeV/nucleon is investigated. The calculated results are in good qualitative agreement with the experimental data which indicated that there were significantly different scalings of the mean number of intermediate mass fragments with the number of neutron and charged particles between the two reaction systems. Meanwhile, it is shown that the preequilibrium emission may affect strongly these scalings. [S0556-2813(99)05911-7]

PACS number(s): 25.70.Pq, 02.70.Ns, 24.10.Lx

Heavy-ion collisions (HIC's) at intermediate and high energies provide a new way to investigate the properties of nuclear matter at high temperature and high density which is connected with the nuclear equation of state (EOS), multifragmentation, and liquid-gas phase transition [1–3]. The nuclear multifragmentation, i.e., the production of several intermediate mass fragments (IMF's), particularly attracts a lot of interest since it constitutes a major decay channel of nuclear matter formed in such heavy-ion collisions [4–7]. Meanwhile, the nuclear multifragmentation offers a unique opportunity to explore the properties of a quantum many-body system very far from equilibrium and to discover the universal law of fragmentation, which are theoretically meaningful for investigating the phase transition and critical phenomenon of a finite system. A great deal of experimental and theoretical work has been devoted to studies of the mechanism of IMF emission and the resulting physical pictures mainly focus on the volume instability from the density fluctuations, thermodynamical instability from the temperature fluctuations, and shape instability from the surface fluctuations [8,2].

In recent years, with the establishment of secondary beam facilities at many laboratories around the world, radioactive beams of nuclei with large neutron or proton excess have been used and heavy-ion physics has opened up a new field, radioactive nuclear beam (RNB) physics. Consequently, one can investigate the properties of nuclei very far from the β stability line and isospin degrees of freedom in nuclear reactions at wide energy ranges for different projectile-target combinations. The isospin effects on preequilibrium nucleon emission [9,10], the isospin nonequilibrium in intermediate energy HIC's [11,12], and the isospin dependence of directed collective flow [13–16] and radial expansion flow [17] have been studied experimentally and theoretically. A recent review can be found in Ref. [18].

More recently, the isospin dependence of nuclear multifragmentation in $^{112}\text{Sn}+^{112}\text{Sn}$ and $^{124}\text{Sn}+^{124}\text{Sn}$ collisions at 40 MeV/nucleon has been observed by the MSU group [19]. This effect was reproduced qualitatively by the expanding

evaporating source (EES) model [20,19] whose cooling rates were dependent on the neutron number of the source. An extensive study of these reactions using the percolation model [21] failed to reproduce this effect. In this work, we report the calculated results for the two reactions based on an isospin-dependent quantum molecular dynamics (IQMD) model. A general review about the QMD model can be found in Ref. [22]. Here the IQMD model includes explicitly isospin degrees of freedom, i.e., isospin-dependent symmetry energy, Coulomb interaction, experimental N - N cross sections, and particularly the isospin-dependent Pauli blocking. This model has been used recently to explain successfully several phenomena in HIC's at intermediate energies, which depend on the isospin of the reaction system [12,16]. In the QMD model, nucleon i is represented by a Gaussian form of wave function:

$$\Psi_i(\mathbf{r}, t) = \frac{1}{(2\pi L)^{3/4}} e^{-[\mathbf{r}-\mathbf{r}_i(t)]^2/(4L)} e^{i\mathbf{p}_i \cdot \mathbf{r}/\hbar}. \quad (1)$$

Performing a Wigner transformation for Eq. (1), we get the nucleon's Wigner density distribution in phase space:

$$f_i(\mathbf{r}, \mathbf{p}, t) = \frac{1}{(\pi\hbar)^3} \exp\left[-\frac{[\mathbf{r}-\mathbf{r}_i(t)]^2}{2L} - \frac{[\mathbf{p}-\mathbf{p}_i(t)]^2 2L}{\hbar^2}\right], \quad (2)$$

where \mathbf{r}_i and \mathbf{p}_i represent the mean position and momentum of the i th nucleon, respectively, which satisfy the canonical equation of motion. The L is the so-called Gaussian wave packet width (here $L=2.0 \text{ fm}^2$). In the IQMD model, the nuclear mean field can be parametrized by

$$U(\rho, \tau_z) = \alpha(\rho/\rho_0) + \beta(\rho/\rho_0)^\gamma + \frac{1}{2}(1-\tau_z)V_c + C \frac{\rho_n - \rho_p}{\rho_0} \tau_z + U^{\text{Yuk}}, \quad (3)$$

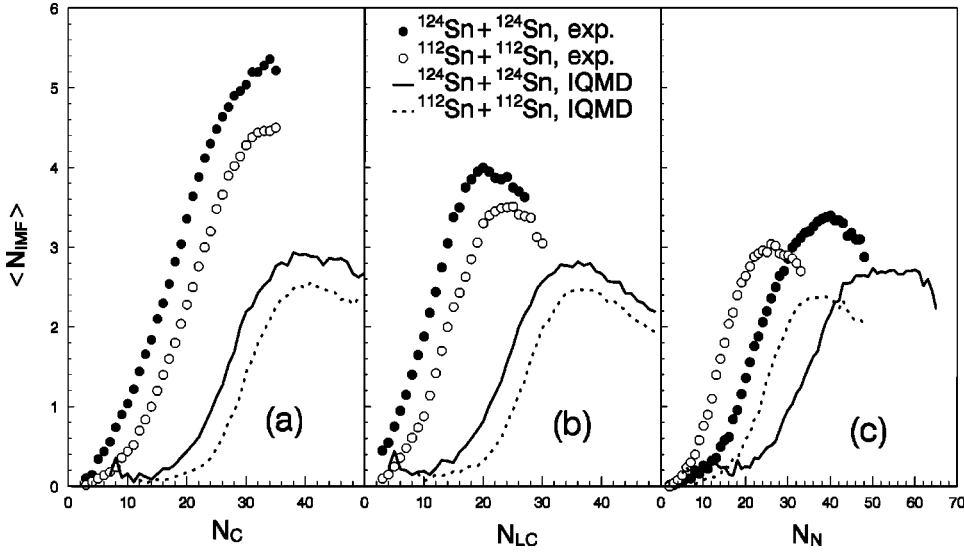


FIG. 1. Average number of intermediate mass fragments (IMF's), $\langle N_{\text{IMF}} \rangle$, versus number of charged particles, N_C (a), light-charged particles with $Z \leq 2$, N_{LC} (b), and neutrons, N_N (c). The solid (open) circles denote the experimental data for the $^{124}\text{Sn} + ^{124}\text{Sn}$ ($^{112}\text{Sn} + ^{112}\text{Sn}$) reaction. The solid (dotted) line represents the IQMD model predictions for the $^{124}\text{Sn} + ^{124}\text{Sn}$ ($^{112}\text{Sn} + ^{112}\text{Sn}$) reaction.

with ρ_0 the normal nuclear matter density (here, 0.16 fm^{-3}); ρ , ρ_n , and ρ_p are the total, neutron, and proton interaction densities, respectively; τ_z is the z th component of the isospin degree of freedom, which equals 1 or -1 for neutrons or protons, respectively; V_c is the Coulomb potential; and U^{Yuk} is Yukawa (surface) potential which has the following form [22]:

$$U^{\text{Yuk}} = \frac{V_Y}{2m} \sum_{i \neq j} \frac{1}{r_{ij}} \exp(Lm^2) [\exp(-mr_{ij}) \text{erfc}(\sqrt{L}m r_{ij} / \sqrt{4L}) - \exp(mr_{ij}) \text{erfc}(\sqrt{L}m + r_{ij} / \sqrt{4L})], \quad (4)$$

with $V_Y = -0.0074 \text{ GeV}$ and $m = 1.25 \text{ fm}^{-1}$. The relative distance $r_{ij} = |\mathbf{r}_i - \mathbf{r}_j|$. In the present work, the so-called soft EOS with an incompressibility of $K = 200 \text{ MeV}$ is used and the symmetry strength $C = 32 \text{ MeV}$.

In the initialization process of the IQMD model, the neutron and proton densities calculated from the nonlinear relativistic mean-field (RMF) theory [23] are used to initialize

the ground states of ^{112}Sn and ^{124}Sn in terms of the Monte Carlo method. Particularly, in the nonlinear RMF calculations we use the latest force parameter NL3 which is able to provide a very good description not only for the properties of stable nuclei but also for those far from the valley of β stability in all cases considered so far [24].

We construct clusters by means of an isospin-dependent modified coalescence model [16,17], in which first particles with relative momenta smaller than P_0 and relative distances smaller than R_0 are coalesced into one cluster (here $R_0 = 3.5 \text{ fm}$ and $P_0 = 300 \text{ MeV}/c$); then we check whether the cluster is or is not an isotope existing in the nuclear data sheets, and if it is, then the cluster can be accepted; finally in order to get rid of nonphysical line-type clusters one should check whether the condition, $R_{\text{rms}} \leq 1.14A^{1/3}$, is or is not satisfied, and if so, the cluster is considered as a valid fragment eventually (here, the R_{rms} and A are the root-mean-square radius and mass number of the cluster, respectively). Therefore, the present model to construct clusters is an extended version of the conventional coalescence model which was adopted in Ref. [16] by considering self-consistently the

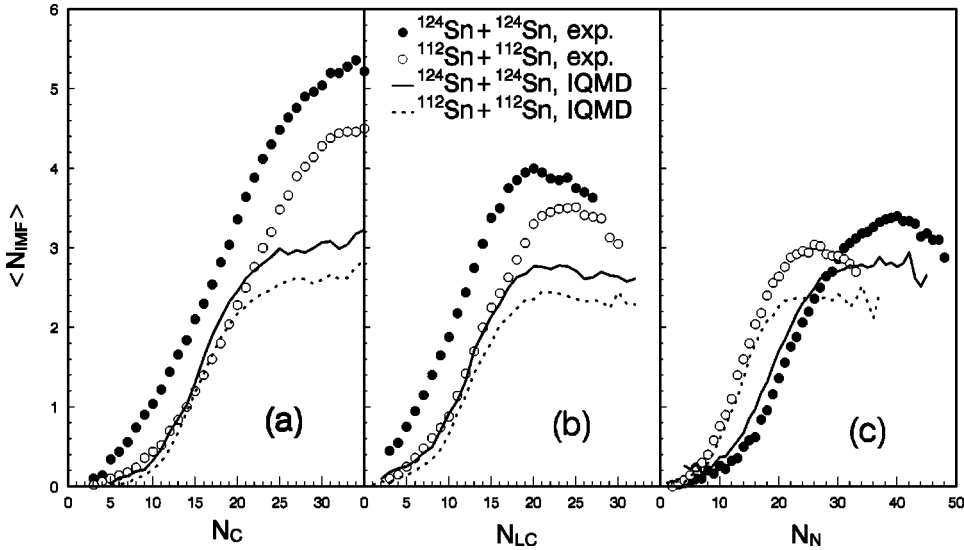


FIG. 2. Same as in Fig. 1 but in the calculated results the pre-equilibrium particles have been excluded.

isospin constraint and aggregation procedure. In the calculations, it is indicated that the present calculated results are insensitive to the selection of either $R_0=3.5$ fm and $P_0=300$ MeV/c or $R_0=2.4$ fm and $P_0=200$ MeV/c, the latter being used in our previous work [16].

In the present calculations, we simply assume that the number of the events is proportional to impact parameter b and $b=1, 2, 3, 4, 5, 6, 7, 8, 9,$ and 10 fm are adopted. The calculation indicates that the number of IMF's has become very small and the multifragmentation mechanism has basically disappeared at $b=10$ fm. To accumulate the numerical statistics, we select the fragments by summing over the fragments of $t \geq 200$ fm/c since the charge distributions have been very stable after 200 fm/c.

Figures 1(a), 1(b), and 1(c) show the average number of IMF's ($\langle N_{\text{IMF}} \rangle$; $3 \leq Z \leq 33$) as a function of number of charged particles, N_C , light-charged particles with $Z \leq 2$, N_{LC} , and neutrons, N_N , respectively. The solid (open) circles denote the experimental data for the $^{124}\text{Sn} + ^{124}\text{Sn}$ ($^{112}\text{Sn} + ^{112}\text{Sn}$) reaction. The solid (dotted) line represents the IQMD model prediction for the $^{124}\text{Sn} + ^{124}\text{Sn}$ ($^{112}\text{Sn} + ^{112}\text{Sn}$) reaction. From Fig. 1, one can see clearly that the IQMD model predictions are in very good agreement with the experimental data in trends; namely, for the same N_C or N_{LC} the $\langle N_{\text{IMF}} \rangle$ for $^{124}\text{Sn} + ^{124}\text{Sn}$ is larger than that for $^{112}\text{Sn} + ^{112}\text{Sn}$. The calculated results indicate that the magnitude of the maxima in different correlations has nearly the same values while the experimental data show different values for the different correlations, which implies that the present IQMD model cannot reproduce this feature of the data. More importantly here, there is agreement between the data and the IQMD model predictions for the magnitude of the isospin effect. In addition, the calculated results cannot reproduce the maxima of $\langle N_{\text{IMF}} \rangle$, which is mainly due to not considering the statistical decay of excited fragments in the reaction final state. Meanwhile, we can see that the calculated results cannot reproduce the positions of the maxima in $\langle N_{\text{IMF}} \rangle$ versus N_C , N_{LC} , or N_N , which is easy to understand since the preequilibrium particles are still included and they contribute to N_C , N_{LC} , or N_N . This problem also exists in calculations of the EES model [19] or percolation model [21]. Therefore, it seems that the preequilibrium emission may play a very important role in these correlations.

If the preequilibrium particles are excluded, then the results can be displayed in Fig. 2 which is the same as Fig. 1 but in the calculations the preequilibrium particles have been excluded. In the present calculations, the preequilibrium particle is simply defined as the light fragment with $Z \leq 2$ which satisfies the following conditions: the relative distance between it and any other fragment is larger than 3.5 fm, the average kinetic energy per nucleon of this fragment is larger than 8 MeV in center-of-mass (c.m.) system, it moves far from the center of mass in the c.m. system, and its relative distance to the center of mass is larger than the root-mean-square radius of the reaction system. From the comparison between Fig. 1 and Fig. 2, we can see clearly that the preequilibrium emission affects strongly the sorting axis, which results in the calculated results reproducing very well the positions of the maxima in $\langle N_{\text{IMF}} \rangle$ versus N_C , N_{LC} , or N_N

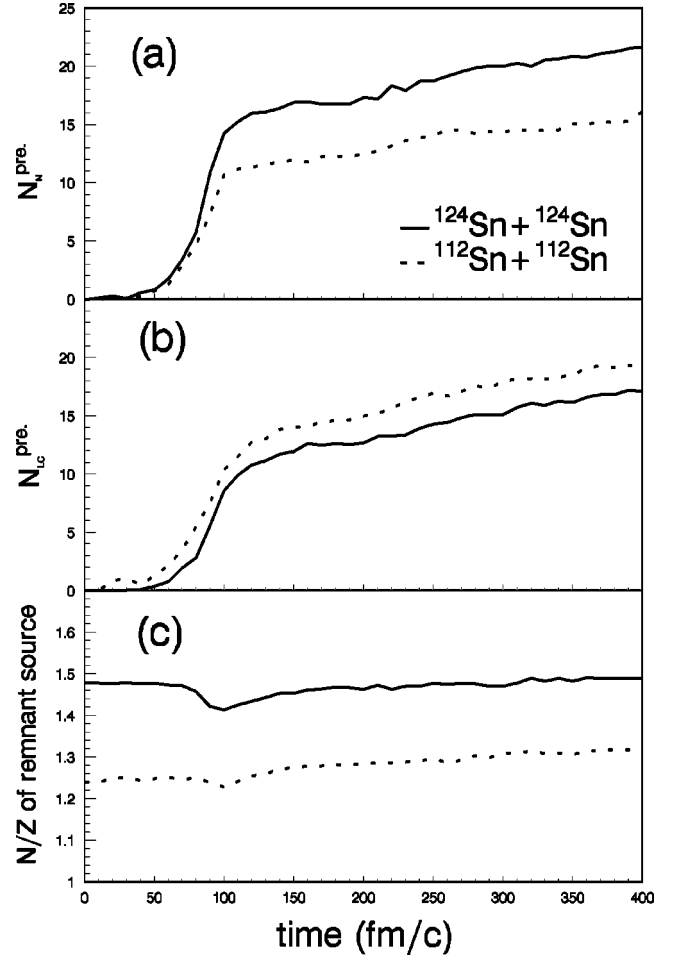


FIG. 3. The IQMD-model-predicted time evolution of number of preequilibrium neutrons, N_N^{pre} (a), light-charged particles, N_{LC}^{pre} (b), and N/Z of the remnant sources (c) for central collisions of systems $^{124}\text{Sn} + ^{124}\text{Sn}$ (solid line) and $^{112}\text{Sn} + ^{112}\text{Sn}$ (dotted line).

although the isospin dependence of the horizontal shifts for the different correlations in Fig. 2 becomes worse than that in Fig. 1 for the peripheral collisions (corresponding to small N_C , N_{LC} , or N_N). This worsening may be a limitation of the present way of determining preequilibrium particles due to the lack of experimental information.

In order to illustrate the influence of the preequilibrium emission on the two reactions, at $b=0$ we display in Figs. 3(a), 3(b), and 3(c) the IQMD-model-predicted time evolution of the number of preequilibrium neutrons (N_N^{pre}), light-charged particles (N_{LC}^{pre}), and N/Z of the remnant sources (here the remnant source is defined as the heavy residue after excluding the preequilibrium particles), respectively. The solid (dotted) line corresponds to the result of $^{124}\text{Sn} + ^{124}\text{Sn}$ ($^{112}\text{Sn} + ^{112}\text{Sn}$). From Figs. 3(a) and 3(b), one can clearly see that nearly all preequilibrium particles are emitted in the time interval from 50 to 100 fm/c for both reactions and the subsequent particle emission is less important. Meanwhile, it is seen that the preequilibrium neutron and light-charged particle emissions are very different for the two systems; i.e., the more neutron-rich system $^{124}\text{Sn} + ^{124}\text{Sn}$ emits more preequilibrium neutrons and fewer preequilibrium light-charged

particles than the system $^{112}\text{Sn}+^{112}\text{Sn}$, and the number of neutrons is larger than that of light-charged particles for $^{124}\text{Sn}+^{124}\text{Sn}$ while the opposite result is observed for $^{112}\text{Sn}+^{112}\text{Sn}$, which may be due to the former having a thick neutron skin. This phenomenon is also observed in the analysis of the EES model [19]. As a matter of fact, the more neutron-rich system $^{124}\text{Sn}+^{124}\text{Sn}$ emits more preequilibrium neutrons to cool and consequently it remains less energetic so as to emit less light-charged particles. In addition, from Fig. 3(c) we can see that N/Z of the remnant sources has changed from the original 1.48 (1.24) to 1.41 (1.23) at 100 fm/c and then 1.49 (1.30) at 400 fm/c, which shows that the preequilibrium emission has a big influence on the N/Z of the remnant source of $^{124}\text{Sn}+^{124}\text{Sn}$ around 100 fm/c. Therefore, the preequilibrium emission affects the N/Z composition of the fragmenting system as expected [21].

It is well known that the total charge contained in fragments with two or more charges, Z_{bound} , is also often measured experimentally and the correlation between $\langle N_{\text{IMF}} \rangle$ and Z_{bound} is usually used to investigate nuclear multifragmentation [25,26]. It should be noted that the preequilibrium light particles have little influence on Z_{bound} since the neutron and hydrogen isotopes do not contribute to the Z_{bound} . The $\langle N_{\text{IMF}} \rangle$ as a function of Z_{bound} is shown in Fig. 4. In the left panel of Fig. 4 the effect of preequilibrium emission is not considered while the preequilibrium particles have been excluded in the right panel of Fig. 4. The solid (open) line represents the IQMD model prediction for the $^{124}\text{Sn}+^{124}\text{Sn}$ ($^{112}\text{Sn}+^{112}\text{Sn}$) collisions. From Fig. 4 we can see that there exists very significantly different scalings of $\langle N_{\text{IMF}} \rangle$ with Z_{bound} between $^{124}\text{Sn}+^{124}\text{Sn}$ and $^{112}\text{Sn}+^{112}\text{Sn}$ collisions; i.e., for a given value of Z_{bound} , a larger $\langle N_{\text{IMF}} \rangle$ is observed for $^{124}\text{Sn}+^{124}\text{Sn}$ than $^{112}\text{Sn}+^{112}\text{Sn}$. Meanwhile, comparison between the left and right panels of Fig. 4 implies that the preequilibrium emission has hardly any influence on the scalings of $\langle N_{\text{IMF}} \rangle$ with Z_{bound} as expected, which indicates that the correlation between $\langle N_{\text{IMF}} \rangle$ and Z_{bound} is more convenient than that between $\langle N_{\text{IMF}} \rangle$ and N_C , N_{LC} , or N_N for a comparison of theoretical calculations and experimental data. Unfortunately, experimental data involving Z_{bound} are not available.

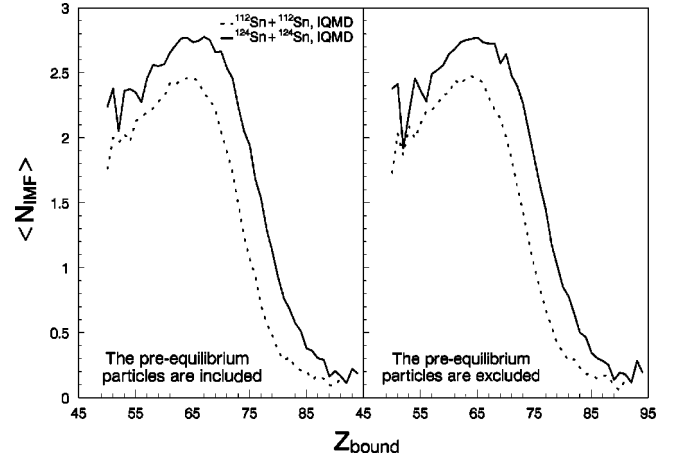


FIG. 4. IQMD model predicted average number of intermediate mass fragments (IMF's), $\langle N_{\text{IMF}} \rangle$, versus the total charge contained in fragments with two or more charges, Z_{bound} , at two different situations: the effect of preequilibrium emission is not considered (left panel) and the preequilibrium particles are excluded (right panel). The solid (dotted) line represents results for the $^{124}\text{Sn}+^{124}\text{Sn}$ ($^{112}\text{Sn}+^{112}\text{Sn}$) collisions.

In conclusion, the experimental data could be reproduced qualitatively within the framework of the IQMD model. In particular, the IQMD model predictions are in quantitative agreement with the experimental data on the magnitude of the isospin effect. The main discrepancy is that the IQMD model cannot reproduce the maxima of $\langle N_{\text{IMF}} \rangle$ mainly due to not considering the statistical decay of excited fragments in the reaction final state. Meanwhile, the IQMD model calculations indicate that preequilibrium emission plays an important role in scaling of the $\langle N_{\text{IMF}} \rangle$ with N_C , N_{LC} , or N_N but has hardly any influence on scalings of $\langle N_{\text{IMF}} \rangle$ with Z_{bound} .

This work was supported by the National Natural Science Foundation of China under Grant Nos. 19609033, 19875068, and 19847002, the Foundation of the Chinese Academy of Sciences, and the Foundation of National Educational Commission of People's Republic of China.

- [1] G. Peilert, H. Stocker, and W. Greiner, Rep. Prog. Phys. **57**, 533 (1994).
- [2] L. G. Moretto and G. J. Wozniak, Annu. Rev. Nucl. Part. Sci. **43**, 379 (1993).
- [3] J. Pochodzalla, T. Mohlenkamp, T. Rubehn, A. Schuttauf, A. Worner, E. Zude, M. Begemann-Blaich, Th. Blaich, H. Emiling, A. Ferrero, C. Gross, G. Imme, I. Iori, G. J. Kunde, W. D. Kunze, V. Lindenstruth, U. Lynen, A. Moroni, W. F. Muller, B. Ocker, G. Raciti, H. Sann, C. Schwarz, W. Seidel, V. Serfling, J. Stroth, W. Trautmann, A. Trzcinski, A. Tucholski, G. Verde, and B. Zwieglinski, Phys. Rev. Lett. **75**, 1040 (1995).
- [4] D. R. Bowman, G. F. Peaslee, R. T. de Souza, N. Carlin, C. K. Gelbke, W. G. Gong, Y. D. Kim, M. A. Lisa, W. G. Lynch, L.

Phair, M. B. Tsang, C. Williams, N. Colonna, K. Hanold, M. A. McMahan, G. J. Wozniak, L. G. Moretto, and W. A. Friedman, Phys. Rev. Lett. **67**, 1527 (1991).

- [5] C. A. Ogilvie, J. C. Adloff, M. Begemann-Blaich, P. Bouissou, J. Hubele, G. Imme, I. Iori, P. Kreuzt, G. J. Kunde, S. Leray, V. Lindenstruth, Z. Liu, U. Lynen, R. J. Meijer, U. Milkau, W. F. Muller, C. Ngo, J. Pochodzalla, G. Raciti, G. Rudolf, H. Sann, A. Schuttauf, W. Seidel, L. Stuttge, W. Trautmann, and A. Tucholski, Phys. Rev. Lett. **67**, 1214 (1991).
- [6] K. Hagel, M. Gonin, R. Wada, J. B. Natowitz, B. H. Sa, Y. Lou, M. Gui, D. Utley, G. Nebbia, D. Fabris, G. Prete, J. Ruiz, D. Drain, B. Chambon, B. Cheynis, D. Guinet, X. C. Hu, A. Demeyer, C. Pastor, A. Giorni, A. Lleres, P. Stassi, J. B. Viano, and P. Gonthier, Phys. Rev. Lett. **68**, 2141 (1992).

- [7] M. B. Tsang, W. C. Hsi, W. G. Lynch, D. R. Bowman, C. K. Gelbke, M. A. Lisa, G. F. Peaslee, G. J. Kunde, M. Begemann-Blaich, T. Hofmann, J. Hubele, J. Kempter, P. Kreuzt, W. D. Kunze, V. Lindenstruth, U. Lynen, M. Mang, W. F. Muller, M. Neumann, B. Ocker, C. A. Ogilvie, J. Pochodzalla, F. Rosenberger, H. Sann, A. Schuttauf, V. Serfling, J. Stroth, W. Trautmann, A. Tucholski, A. Worner, E. Zude, B. Zwieglinski, S. Aiello, G. Imme, V. Pappalardo, G. Raciti, R. J. Charity, L. G. Sobotka, I. Iori, A. Moroni, R. Scardaoni, A. Ferrero, W. Seidel, Th. Blaich, L. Stuttge, A. Cosmo, W. A. Friedman, and G. Peilert, *Phys. Rev. Lett.* **71**, 1502 (1993).
- [8] F. S. Zhang and L. X. Ge, *Nuclear Multifragmentation* (Science Press, Beijing, 1998).
- [9] L. W. Chen, X. D. Zhang, and L. X. Ge, *High Energy Phys. Nucl. Phys.* **20**, 1091 (1996); *ibid.* (overseas edition) **21**, 486 (1997).
- [10] B. A. Li, C. M. Ko, and Z. Z. Ren, *Phys. Rev. Lett.* **78**, 1644 (1997).
- [11] B. A. Li and S. J. Yennello, *Phys. Rev. C* **52**, R1746 (1995).
- [12] L. W. Chen, L. X. Ge, X. D. Zhang, and F. S. Zhang, *J. Phys. G* **23**, 211 (1997).
- [13] B. A. Li, Z. Z. Ren, C. M. Ko, and S. J. Yennello, *Phys. Rev. Lett.* **76**, 4492 (1996).
- [14] R. Pak, W. Benenson, O. Bjarki, J. A. Brown, S. A. Hannuschke, R. A. Lacey, B. A. Li, A. Nadasen, E. Norbeck, P. Pogodin, R. E. Russ, M. Steiner, N. T. B. Stone, A. M. Vander Molen, G. D. Westfall, L. B. Yang, and S. J. Yennello, *Phys. Rev. Lett.* **78**, 1022 (1997).
- [15] R. Pak, B. A. Li, W. Benenson, O. Bjarki, J. A. Brown, S. A. Hannuschke, R. A. Lacey, D. J. Magestro, A. Nadasen, E. Norbeck, R. E. Russ, M. Steiner, N. T. B. Stone, A. M. Vander Molen, G. D. Westfall, L. B. Yang, and S. J. Yennello, *Phys. Rev. Lett.* **78**, 1026 (1997).
- [16] L. W. Chen, F. S. Zhang, and G. M. Jin, *Phys. Rev. C* **58**, 2283 (1998).
- [17] L. W. Chen, F. S. Zhang, G. M. Jin, and Z. Y. Zhu, *Phys. Lett. B* **459**, 21 (1999).
- [18] B. A. Li, C. M. Ko, and W. Bauer, *Int. J. Mod. Phys. E* **7**, 147 (1998).
- [19] G. J. Kunde, S. J. Gaff, C. K. Gelbke, T. Glasmacher, M. J. Huang, R. Lemmon, W. G. Lynch, L. Manduci, L. Matin, M. B. Tsang, W. A. Friedman, J. Dempsey, R. J. Charity, L. G. Sobotka, D. K. Agnihotri, B. Djerrou, W. U. Schroder, W. Skulski, J. Toke, and K. Wyrozowski, *Phys. Rev. Lett.* **77**, 2897 (1996).
- [20] W. A. Friedman, *Phys. Rev. Lett.* **60**, 2125 (1988); *Phys. Rev. C* **42**, 667 (1990).
- [21] G. Kortemeyer, W. Bauer, and G. D. Kunde, *Phys. Rev. C* **55**, 2730 (1997); W. Bauer, D. R. Dean, U. Mosel, and U. Post, *Phys. Lett.* **150B**, 53 (1985).
- [22] J. Aichel, *Phys. Rep.* **202**, 233 (1991).
- [23] Z. Y. Zhu, W. Q. Shen, Y. H. Cai, and Y. G. Ma, *Phys. Lett. B* **328**, 1 (1994).
- [24] G. A. Lalazissis, J. Konig, and P. Ring, *Phys. Rev. C* **55**, 540 (1997).
- [25] P. Kreuzt, J. C. Adloff, M. Begemann-Blaich, P. Bouissou, J. Hubele, G. Imme, I. Iori, G. J. Kunde, S. Leray, V. Lindenstruth, Z. Liu, U. Lynen, R. J. Meijer, U. Milkau, A. Moroni, W. F. Muller, C. Ngo, C. A. Ogilvie, J. Pochodzalla, G. Raciti, G. Rudolf, H. Sann, A. Schuttauf, W. Seidel, L. Stuttge, W. Trautmann, and A. Tucholski, *Nucl. Phys.* **A556**, 672 (1993).
- [26] J. Pochodzalla, S. Aiello, M. Begemann-Blaich, Th. Blaich, D. R. Bowman, R. J. Charity, A. Cosmo, A. Ferrero, C. K. Gelbke, W. C. Hsi, J. Hubele, G. Imme, I. Iori, J. Kempter, P. Kreuzt, G. J. Kunde, W. D. Kunze, V. Lindenstruth, M. A. Lisa, W. G. Lynch, U. Lynen, M. Mang, L. G. Moretto, A. Moroni, W. F. Muller, M. Neumann, B. Ocker, C. A. Ogilvie, V. Pappalardo, G. F. Peaslee, G. Raciti, F. Rosenberger, T. Rubehn, H. Sann, R. Scardaoni, A. Schuttauf, W. Seidel, V. Serfling, L. G. Sobotka, J. Stroth, L. Stuttge, W. Trautmann, M. B. Tsang, A. Tucholski, C. Williams, A. Worner, E. Zude, and B. Zwieglinski, *Nucl. Phys.* **A583**, 553c (1995).